A Kv3-like persistent, outwardly rectifying, Cs^+-permeable, K^+ current in rat subthalamic nucleus neurones

Mark A. Wigmore and Michael G. Lacey

Department of Pharmacology, Division of Neuroscience, The Medical School, University of Birmingham, Vincent Drive, Edgbaston, Birmingham B15 2TT, UK

(Received 6 April 2000; accepted after revision 21 June 2000)

1. A persistent outward K^+ current (I_{PO}), activated by depolarization from resting potential, has been identified and characterized in rat subthalamic nucleus (SThN) neurones using whole-cell voltage-clamp recording in brain slices.

2. I_{PO} both rapidly activated ($\tau = 8$ ms at $+5$ mV) and deactivated ($\tau = 2$ ms at -68 mV), while showing little inactivation. Tail current reversal potentials varied with extracellular K^+ concentration in a Nernstian manner.

3. Intracellular Cs^+ did not alter either I_{PO} amplitude or the voltage dependence of activation, but blocked transient (A-like) outward currents activated by depolarization. When extracellular K^+ was replaced with Cs^+, I_{PO} tail current reversal potentials were dependent upon the extracellular Cs^+ concentration, indicating an ability to conduct Cs^+, as well as K^+.

4. I_{PO} was blocked by Ba^{2+} (1 mM), 4-aminopyridine (1 mM) and tetraethylammonium (TEA; 20 mM), with an IC_{50} for TEA of 0·39 mM.

5. The I_{PO} conductance appeared maximal (38 nS) at around $+27$ mV, half-maximal at -13 mV, with the threshold for activation at around -38 mV.

6. TEA (1 mM) blocked the action potential after-hyperpolarization and permitted accommodation of action potential firing at frequencies greater than around 200 Hz.

7. We conclude that I_{PO}, which shares many characteristics of currents attributable to Kv3.1 K^+ channels, enables high-frequency spike trains in SThN neurones.

The subthalamic nucleus (SThN) is a small, densely packed nucleus situated in the ventral midbrain. It contains neurones making glutamatergic projections primarily to the external segment of the globus pallidus and substantia nigra pars reticulata (Albin *et al.* 1989; Parent & Hazrati, 1995). The importance of these projections to other basal ganglia nuclei has become increasingly appreciated in recent years. Thus, not only can lesions of the SThN produce the hyperkinetic syndrome of ballism (Guridi & Obeso, 1997), but also the akinesia in animal models of Parkinson's disease can be ameliorated by SThN lesions (Bergman *et al.* 1990; Wichmann *et al.* 1994*b*). Moreover, surgical SThN lesions have proved beneficial in Parkinson's disease (Krack *et al.* 1999) and similar benefits may be obtained by bilateral high-frequency stimulation of the SThN (Benazzouz *et al.* 1993; Limousin *et al.* 1995; Krack *et al.* 1999), which has been proposed to inactivate SThN neurones by depolarization block (Benazzouz *et al.* 1993; Limousin *et al.* 1995). In animal models of akinesia or dyskinesia of basal ganglia origin, cells in several of the component nuclei, including the SThN, display an increased tendency to fire synchronously which, in parkinsonian models, is associated with an increased tendency to fire in bursts (Bergman *et al.* 1994; Hassani *et al.* 1996; Wichmann & Delong, 1996). This change in firing pattern probably results from increased input convergence, reflecting breakdown of separation of 'channels' of sensorimotor information, processed in parallel within the cortico-basal ganglia-thalamo-cortical circuit (Alexander *et al.* 1990; Wichmann & Delong, 1996; Brown & Marsden, 1998). The pivotal role of the SThN in this circuit, where its activation seems able to curtail execution of ongoing motor tasks (Delong, 1990), provides the context in which an understanding of the mechanisms that pattern SThN neurone firing might be applied to better understand – and manipulate – extrapyramidal motor function.

In our examination of the cellular mechanisms that govern firing patterns of SThN neurones we, and others (Beurrier *et al.* 1999; Bevan & Wilson, 1999), have employed whole-cell patch recording from brain slice preparations. In the course of our studies we have observed a large persistent outward current (I_{PO}) activated by depolarization from resting potential, whose properties we describe here. SThN neurones are capable of firing at frequencies in excess of 300 Hz *in*

vitro (Nakanishi *et al.* 1987), and can respond with transient, high-frequency bursts in association with limb or eye movements *in vivo* (Matsumara *et al.* 1992; Wichmann *et al.* 1994*a*). Other fast-firing neuronal types, including those of the medial nucleus of the trapezoid body (Brew & Forsythe, 1995; Wang *et al.* 1998*b*), and cortical (Erisir *et al.* 1999) and hippocampal (Du *et al.* 1996; Martina *et al.* 1998) interneurones, also have persistent outwardly rectifying K^+ currents, in many cases attributed to expression of the K^+ channel Kv3.1, which serve to facilitate rapid action potential firing. We present evidence for I_{PO} being an outwardly rectifying K^+ current that operates to restrict action potential duration and accommodation, enabling sustained firing at high frequencies. Our biophysical and pharmacological description of its characteristics invites comparison with the properties of expressed K^+ channels of known molecular sequence. Some of these results have been reported previously in abstract form (Wigmore & Lacey, 1999).

METHODS

Parasagittal slices of rat ventral midbrain were prepared from Wistar rats (70–130 g) as described previously (Miyazaki & Lacey, 1998). Briefly, animals were anaesthetized using 3·5% halothane ('Fluothane') in oxygen, followed by cervical dislocation, in accordance with the Animals (Scientific Procedures) Act, 1986, UK. Brains were quickly removed (within 3 min) into ice-cold artificial cerebrospinal fluid (aCSF) comprising (mM): NaCl, 126; KCl, 3; $CaCl_2$, 1; $MgCl_2$, 5; NaH_2PO_4, 1·2; D-glucose, 20; $NaHCO_3$, 26; and lactate, 4. Slices of 300 μm thickness were cut on a DTK-1000 tissue slicer (Dosaka, Kyoto, Japan) and transferred to a storage chamber or placed directly under a microscope (see below), where they were submerged in aCSF comprising (mM): NaCl, 126; KCl, 2·5; $CaCl_2$, 2·4; $MgCl_2$, 1·3; NaH_2PO_4, 1·2; D-glucose, 10; $NaHCO_3$, 26; continuously bubbled with 95% O_2–5% CO_2 and warmed to 30 °C. Slices were stored thus for at least 30 min prior to commencing recording.

Recording pipettes (resistance, 3–5 MΩ) were pulled from 1·2 mm external diameter borosilicate glass (Clark ElectroMedical, Pangbourne, UK) on a horizontal puller (P-97, Sutter Instruments). Pipettes were filled with a solution containing (mM): either potassium or caesium gluconate, 125; NaCl, 10; $CaCl_2$, 1; $MgCl_2$, 2; BAPTA, 1; Hepes, 10; buffered to pH 7·3–7·4 with either KOH or CsOH. ATP (2 mM) and GTP (0·3 mM) were added on the day of recording from frozen aliquots dissolved in water. For recordings, slices were placed on the base of a bath (volume, $< 0{\cdot}5$ ml) and continuously superperfused (> 2 ml min^{-1}) with aCSF of the same composition as that used for the storage of slices. Experiments were performed at 32 °C, unless stated otherwise. The slice was stabilized by placing a titanium grid (Agar Scientific, UK) across the SThN and holding it down with flattened platinum wire (Goodfellow, UK). Drugs were applied by a gravity-fed system in which one solution was exchanged for another differing only in the one constituent; the dead time before the bath was reached was 20–30 s. CsCl, tetraethylammonium chloride (TEA), 4-amino-pyridine (4-AP), $BaCl_2$ and 4-ethylphenylamino-1,2-dimethyl-6-methylaminopyrimidium chloride (ZD7288) were purchased from Sigma Chemicals (Poole, UK), and tetrodotoxin (TTX) was obtained variously from Sigma, Tocris Cookson Ltd (Bristol, UK) or Alamone Labs Ltd (Jerusalem, Israel). The 'low-Ca^{2+} aCSF' contained 0·24 mM $CaCl_2$, with [$MgCl_2$] raised to 10 mM.

Single cells were visualized for recording using infrared differential interference contrast ('Nomarski') optics with an Olympus BX50WI microscope with ×40 objective, connected to a CCD camera (KP-M1, Hitachi, Tokyo, Japan) and Sony monitor. The image intensity was boosted using a digital constrast enhancer (CE-4, Brian Reece Scientific, Newbury, UK). The SThN could be observed using a low-power objective as a small, dark region on the ventral surface of the brain, bounded by the internal capsule, thalamus and substantia nigra. Whole-cell recordings were made by advancing the recording pipettes slowly into the slice under visual control using a piezoelectric manipulator (PCS-5000, Burleigh Instruments, Fishers, USA), mounted on a Gibraltar stage (Burleigh Instruments). Following formation by suction of a gigaohm seal, the whole-cell recording configuration was attained by applying additional negative pressure to the pipette. All voltage-clamp recordings were made using an Axopatch 1D amplifier, while current-clamp measurements were made with an Axopatch 200A amplifier (both Axon Instruments, CA, USA). Signals were filtered at 1–5 kHz, and data were acquired using pCLAMP software (version 6; Axon Instruments) running on a PC. Series resistances were in the range 4–20 MΩ and were compensated by 60–80%. Whole-cell capacitance was in the range 10–20 pF when K^+ was the principal intra-pipette cation, and 15–30 pF when Cs^+ was used. Series resistance was monitored at least once every 5 min during recordings and cells were discarded if the uncompensated series resistance rose above 25 MΩ. At the end of the experiment the pipette was removed clear of the cell surface whilst still in the superfusate and any DC offset potential noted; membrane potentials were corrected for this offset retrospectively. Membrane potentials are generally reported without compensation for liquid junction potentials (LJPs), except for those given in the Summary, and where stated specifically elsewhere, when a correction of +8 mV was made. Membrane currents were subjected to leak subtractions to remove the passive component of the membrane conductance; this was performed on-line using a $P/4$ or $P/5$ protocol using pCLAMP, and currents are shown leak subtracted unless otherwise stated in the text.

Experimental data were extracted and analysed using Clampfit (pCLAMP suite). Further data analysis was performed with MS-Excel 98 and plotted using Origin 5.0 (MicroCal). The depression of I_{PO} by TEA (expressed as a percentage) was quantified as $[1 - (I_{TEA}/I_{control})] \times 100$, where I_{TEA} and $I_{control}$ are the mean I_{PO} amplitudes in TEA and under control conditions, respectively, calculated as the mean from three separate trials. To construct the concentration–effect plot, the following equation was used for fitting (by Origin), and iterated until the χ^2 value reached a minimum:

$$y = [(A_1 - A_2)/1 + (x/x_0)^p] + A_2,$$

where A_1 and A_2 are the minimum and maximum y values, respectively, p is the slope and x_0 the IC_{50}. Curve fitting was performed off-line using Clampfit, except for current activation curves, for which Origin was employed. The equation used for the activation plot was a Boltzmann equation of the form:

$$y = [(A_1 - A_2)/1 + \exp((x - x_0)/dx)] + A_2,$$

where A_1 and A_2 are the minimum and maximum membrane conductances, respectively, x_0 is the midpoint voltage and dx is the slope. All pooled data are expressed as means ± standard error of the mean (S.E.M.).

RESULTS

Data presented here were obtained from recordings from 56 cells, using either caesium gluconate- ($n = 33$) or potassium gluconate ($n = 23$)-based pipette solutions.

Characteristics of SThN neurones using potassium gluconate-based pipette solution

SThN neurones commonly showed spontaneous action potential firing after whole-cell access was gained with potassium gluconate-based pipette solution (Fig. 1*A*), with a mean firing frequency in the first 2 min of recording of $19{\cdot}5 \pm 6{\cdot}4$ Hz ($n = 7$). However, spontaneous firing was commonly lost after several minutes of whole-cell dialysis. Under these conditions the input resistance was $520{\cdot}8 \pm 78{\cdot}1$ MΩ ($n = 10$), estimated from a voltage step from −60 to −70 mV under voltage-clamp conditions. Cells showed a small time-dependent inward current (attributable to the hyperpolarization-activated inward current, I_h) when stepped to membrane potentials negative to −75 mV under voltage clamp (Fig. 1*B*). They also often demonstrated a region of negative slope conductance positive to −45 mV (Fig. 1*B* and *C*). These properties correspond to other descriptions of SThN neurones (Nakanishi *et al.* 1987; Beurrier *et al.* 1999; Bevan & Wilson, 1999). In the presence of TTX (0·5–1 μM) and low-Ca^{2+} aCSF, spontaneous firing and inward currents activated by depolarization were abolished. Under these conditions, outward currents activated by depolarization were examined using voltage-clamp recording.

Depolarization activates a persistent outward K^+ current

Depolarizing steps from holding potentials in the region of −50 to −60 mV resulted in the activation of a large and sustained outward current that activated at potentials positive to around −30 mV (Fig. 2). This persistent outward current (I_{PO}) showed little inactivation over several hundred milliseconds, even when the membrane potential was stepped to 0 mV. However, it is likely that with potassium gluconate-based pipette solution this current was contaminated with other outward currents. Indeed, a transient A-like component was observed, particularly when the membrane was depolarized from a more negative potential (−80 mV; Fig. 2).

In order to study I_{PO} further, tail currents observed on current deactivation were examined. Families of tail currents were elicited by stepping the membrane potential from −50 mV to between −10 and −16 mV for 500 ms (to

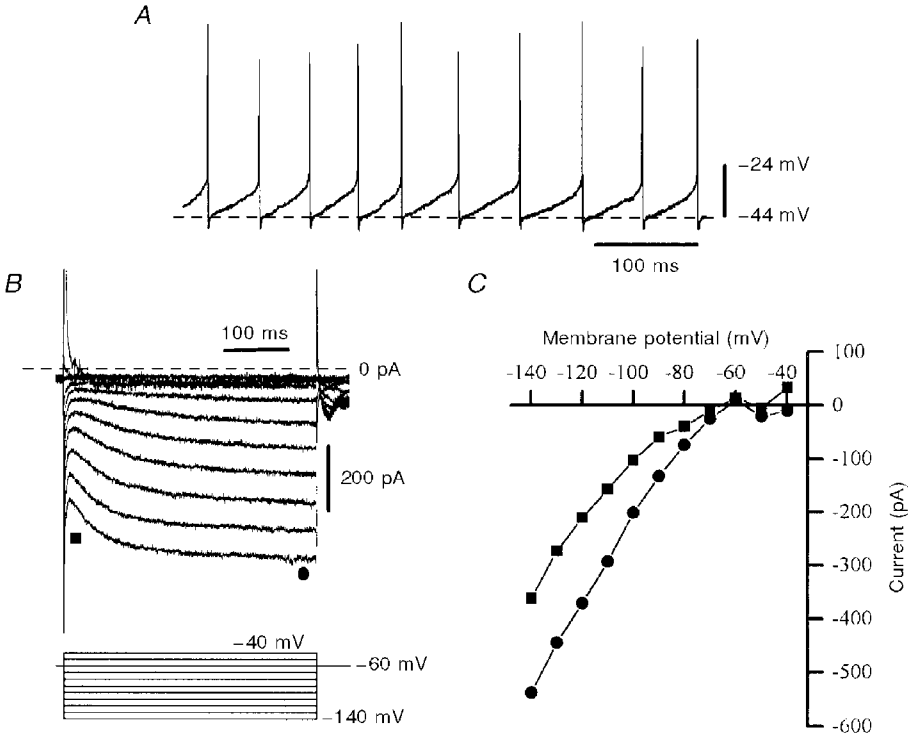

Figure 1. Basic properties of SThN neurones recorded with potassium gluconate-based pipette solution

A, voltage recording showing spontaneous action potential firing (at 20 Hz) at rest. Full spike amplitude is inaccurately displayed due to sampling frequency limitations. *B*, membrane currents (upper records) evoked in another SThN neurone by voltage steps from −60 mV to potentials in the range −140 to −40 mV (lower records). *C*, current–voltage relationships displaying both the instantaneous current (■) and the steady-state current (●) derived from the voltage steps in *B* – the difference may be attributed to I_h. Currents were not leak subtracted.

allow transient currents to inactivate), before hyperpolarizing to potentials in the range −20 to −80 mV. Tail current amplitudes were estimated as the difference between the instantaneous current and steady-state current, as illustrated in Fig. 3*A*. To facilitate these measurements, ZD7288 (50–100 μM), a blocker of I_h, was added to the superfusate, and experiments were performed at room temperature (22–25 °C). Using extracellular K^+ concentrations ($[K^+]_o$) of 5, 10, 15 and 30 mM, mean reversal potentials (V_{rev}) of −62·0 ± 1·8, −53·7 ± 0·9, −43·8 ± 1·5 and −33·0 ± 2·8 mV (n = 3–6 cells), respectively, were obtained (Fig. 3*B* and *C*). Indeed, after LJP correction, these mean values were within +5 mV of those predicted by the Nernst equation for a pure K^+ conductance, except that for the lowest $[K^+]_o$ used (5 mM; +11 mV difference), where V_{rev} was least easy to measure (see Fig. 3*A*). The relationship between V_{rev} and $[K^+]_o$, particularly at the higher $[K^+]_o$ used, also closely approximated that predicted by the Nernst equation if I_{PO} was a pure K^+ conductance (Fig. 3*C*).

I_{PO} can be carried by Cs^+

In an attempt to block I_{PO}, recordings were made with a caesium gluconate-based pipette solution, as many K^+ channels are blocked by internal Cs^+ ions. Under these conditions, the majority (> 90 %) of cells showed spontaneous firing immediately after whole-cell access was gained, but within 1 min depolarized to and subsequently maintained a potential of between −20 and −30 mV, presumably a result of blockade of K^+ channels contributing to the leak conductance. Again, in the presence of TTX (0·5 μM) and low-Ca^{2+} aCSF, to block inward currents, I_{PO} was still evident (Fig. 4). Comparison of pooled data from cells recorded under these conditions (n = 9) and data from cells recorded with potassium gluconate-based pipette solutions (n = 7) showed that neither I_{PO} amplitude nor the voltage dependence of its activation was altered by internal Cs^+ (Fig. 4*B*). The persistence of I_{PO} in the absence of internal K^+ ions indicated that this current could also be carried by Cs^+ ions. This was investigated further by examination of tail currents using Cs^+-based pipette solutions, and with extracellular K^+ replaced with Cs^+. Due to the improved voltage control of the cell membrane when caesium gluconate was used in the pipette, these experiments were performed at 32 °C. The membrane potential was depolarized to between −10 and −26 mV to activate I_{PO} and then stepped to potentials in the range −100 to −106 mV in the presence of $[Cs^+]_o$ (10, 20 or 30 mM) in K^+-free aCSF (Fig. 5*A*). The use of extracellular Cs^+ blocked I_h, obviating the need for ZD7288. Replacement of K^+ with Cs^+ ions as charge carrier gave a slope value of +45 mV per 10-fold change in $[Cs^+]_o$ (estimated by linear regression from data pooled from 7 experiments; Fig. 5*B*). The Nernst equation predicts this slope value to be +60 mV for a completely Cs^+-selective conductance, suggesting that under these conditions Cs^+ ions are the principal, but perhaps not the only, charge carrier. The values for the tail current reversal potentials for each $[Cs^+]_o$ examined (Fig. 5*B*), once corrected for LJP, deviated increasingly negatively from the predicted equilibrium potential for Cs^+ (E_{Cs}) with higher $[Cs^+]_o$ (by up to −8 mV with 30 mM). Thus in addition to using K^+ as the major permeant ion, it appears that I_{PO} can equally well carry Cs^+, depending on cation availability.

Pharmacology of I_{PO}

To characterize I_{PO} further, its sensitivity to various K^+ channel blockers was tested. Using low-Ca^{2+} aCSF and caesium gluconate-based pipette solutions, the membrane potential was held at around −50 mV and stepped by positive increments to around +10 mV to activate I_{PO}. The

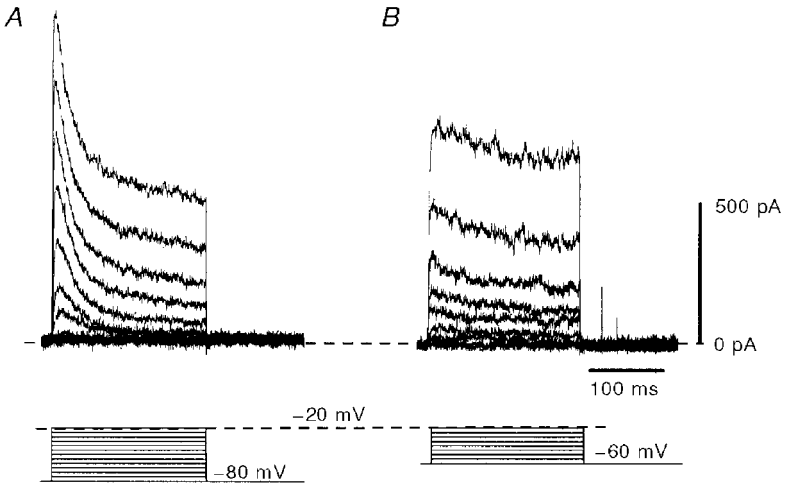

Figure 2. Depolarizing voltage steps elicited a persistent outward current, I_{PO}

A, steps from a holding potential of −80 mV (lower records) resulted in an outward current with both a transient and steady-state component (upper records). *B*, changing the holding potential to −60 mV (lower records) markedly reduced the transient component of the outward current (upper records). Currents were recorded from the same cell using a potassium gluconate-based pipette solution in low-Ca^{2+} aCSF containing TTX (0·5 μM).

effect of three K^+ channel blockers – TEA (20 mM), $BaCl_2$ (1 mM) and 4-AP (1 mM) – were evaluated by measuring their effect on the amplitude of I_{PO} activated at +10 mV. TEA (20 mM) reduced I_{PO} by 98·1 ± 1·4% ($n = 3$; Fig. 6*A*), while $BaCl_2$ (1 mM) and 4-AP (1 mM) depressed I_{PO} by 76·4 ± 8·0 and 90·0 ± 2·2%, respectively ($n = 3$ in both cases; data not shown). Some washout of the effect of TEA was observed, but this was not complete (Fig. 6*A*). Blockade with TEA appeared to be voltage independent (Fig. 6*B*). In an additional series of experiments the potency of TEA was determined. Prior to delivering a test voltage step from around −50 mV to around +10 mV once every 15 s, from which I_{PO} was measured, the membrane potential was held at −80 mV for 1 s, followed by 1 s at −50 mV. Cells were tested with cumulative applications of 0·1, 1 and 10 mM TEA (Fig. 6*C*) or 0·3, 3 and 20 mM TEA ($n = 3$ cells in each group). The degree of depression of (leak-subtracted) current amplitude relative to control was determined and pooled to derive a mean value for each TEA concentration tested. These could be fitted to a logistic concentration–effect curve with a slope value of 0·97, suggesting that TEA is binding to a single site, with an IC_{50} of 0·39 mM (Fig. 6*D*).

I_{PO} activation

Using caesium gluconate-based pipette solution in the presence of $[Cs^+]_o$ (10 mM) and no extracellular K^+, I_{PO} was elicited by depolarizations in the approximate range −50 to +60 mV in six cells. The conductance (G_{PO}) for each voltage step was calculated using the peak (non-inactivated) leak-subtracted current, and normalized by dividing by $V - E_{Cs}$ to account for the driving force on the ion; E_{Cs} was assumed to be −66 mV, as predicted by the Nernst equation. This

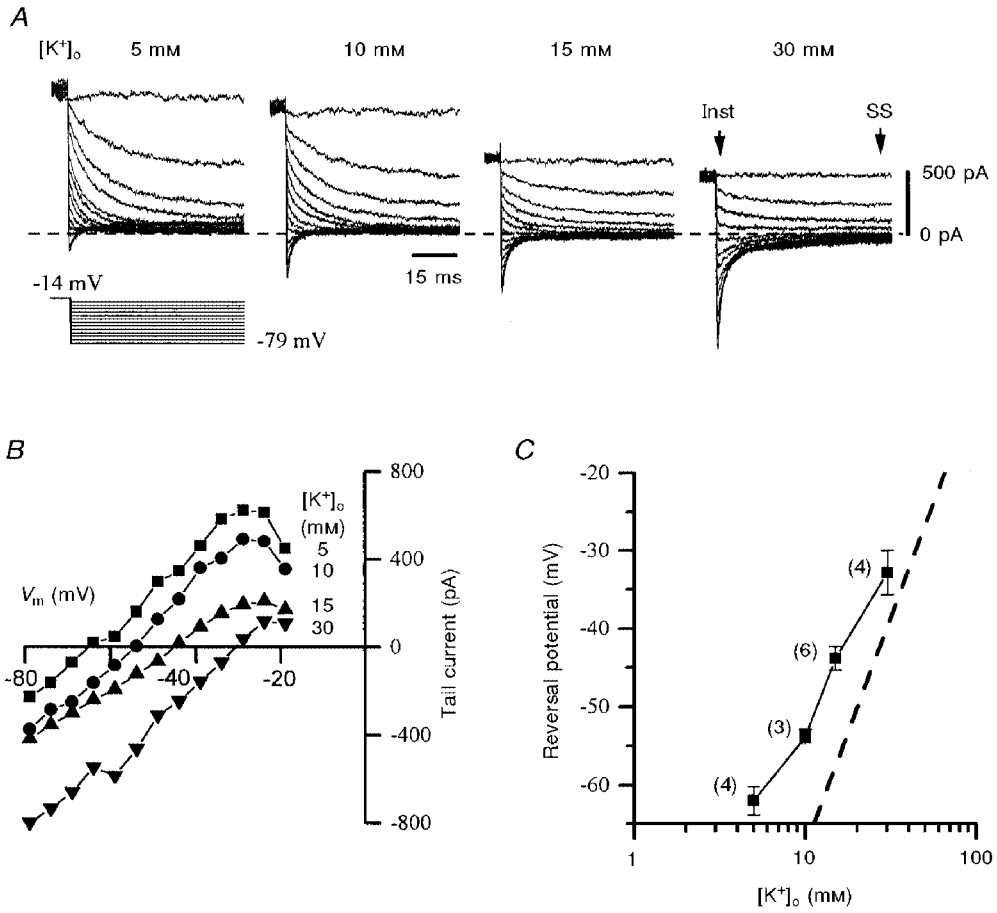

Figure 3. Tail current reversal potentials indicate that I_{PO} is mediated by K^+ ions

A, tail currents recorded in 4 different $[K^+]_o$ as indicated. I_{PO} was initially activated with a 500 ms step to −14 mV, which also allowed any transient currents to inactivate (not shown), and subsequently deactivated by the voltage protocol shown in the lower panel. Tail current amplitude is the difference between the instantaneous (Inst) and steady-state (SS) current, shown for 30 mM $[K^+]_o$, recorded at the start and end of the hyperpolarizing step, respectively. Currents were leak subtracted and recorded at room temperature in low-Ca^{2+} aCSF additionally containing TTX (0·5 μM) and ZD7288 (50 μM). Records are all from the same cell. *B*, plot of tail current amplitude *versus* membrane potential (V_m) derived from records in *A*. *C*, pooled data (means ± S.E.M.) from several such experiments (numbers in parentheses) showing estimated V_{rev} plotted against $[K^+]_o$ on a semilogarithmic scale. The slope predicted by the Nernst equation for a pure K^+ conductance (59 mV per 10-fold change in $[K^+]_o$) is shown by the dashed line, and closely approximates that of the data points.

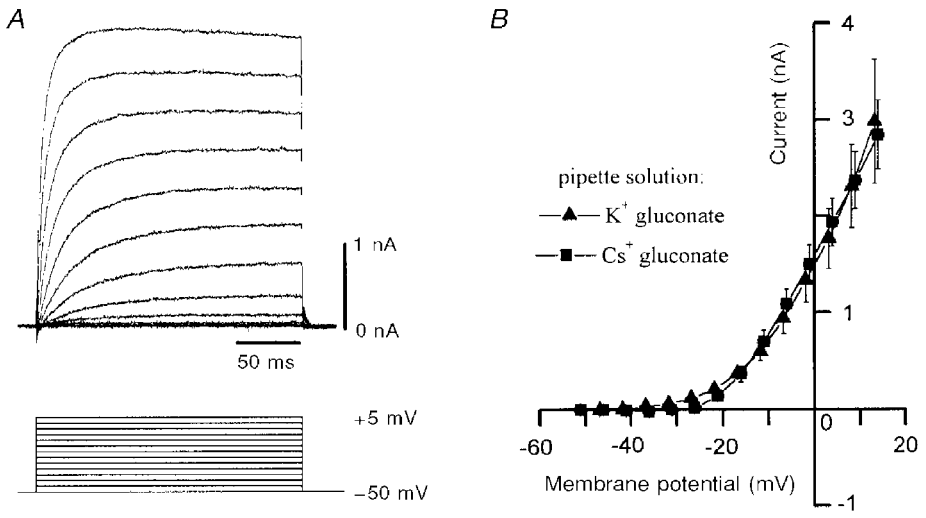

Figure 4. I_{PO} persists in cells recorded using caesium gluconate-filled pipettes

A, upper records: currents resulting from the voltage steps shown in the lower panel in a cell recorded with a caesium gluconate-filled pipette in low-Ca^{2+} aCSF containing TTX (0·5 μM). *B*, data pooled from several cells obtained in experiments such as that in *A* comparing the peak I_{PO} recorded using potassium gluconate- (▲; $n = 7$) or caesium gluconate (■; $n = 9$)-filled pipettes over a range of membrane potentials. There was no difference in activation threshold or current amplitude. Data were obtained under identical conditions except for the intracellular cation; slices were bathed in low-Ca^{2+} aCSF containing TTX (0·5 μM).

permitted a Boltzmann plot of peak G_{PO} with respect to membrane voltage, which describes the voltage dependence of I_{PO} activation (see Methods; Fig. 7). The threshold for current activation occurred at around −30 mV. However, the plot obtained did not reach an asymptote at positive potentials, but rather the conductance continued to increase with depolarization (Fig. 7*B*). This may reflect an inability to reliably control membrane potential in the dendritic tree,

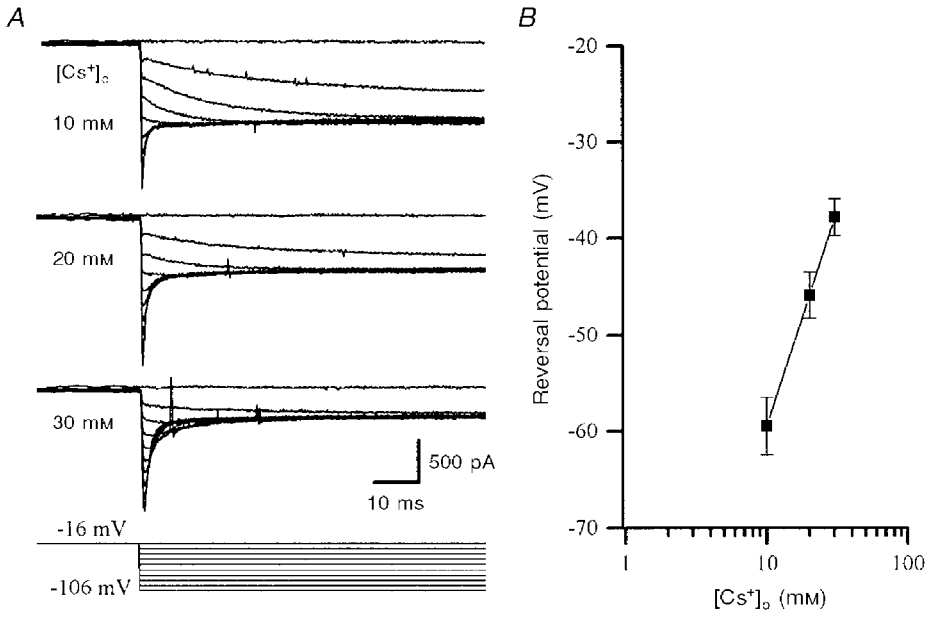

Figure 5. I_{PO} tail current reversal potentials indicate that Cs^+ can also act as the principal permeant cation

A, tail currents recorded from the same cell using a caesium gluconate-filled pipette, in 10, 20 and 30 mM $[Cs^+]_o$ (upper three panels), produced by the voltage steps indicated in the bottom panel. The tail currents reversed polarity at more depolarized potentials as $[Cs^+]_o$ was increased. Currents were leak subtracted and recorded at 32 °C, in the presence of low-Ca^{2+} aCSF and TTX (0·5 μM), in the absence of extracellular K^+. *B*, pooled data (means ± S.E.M.) from 7 such experiments. Tail current reversal potentials were dependent upon $[Cs^+]_o$, showing a 45 mV shift per 10-fold change in $[Cs^+]_o$.

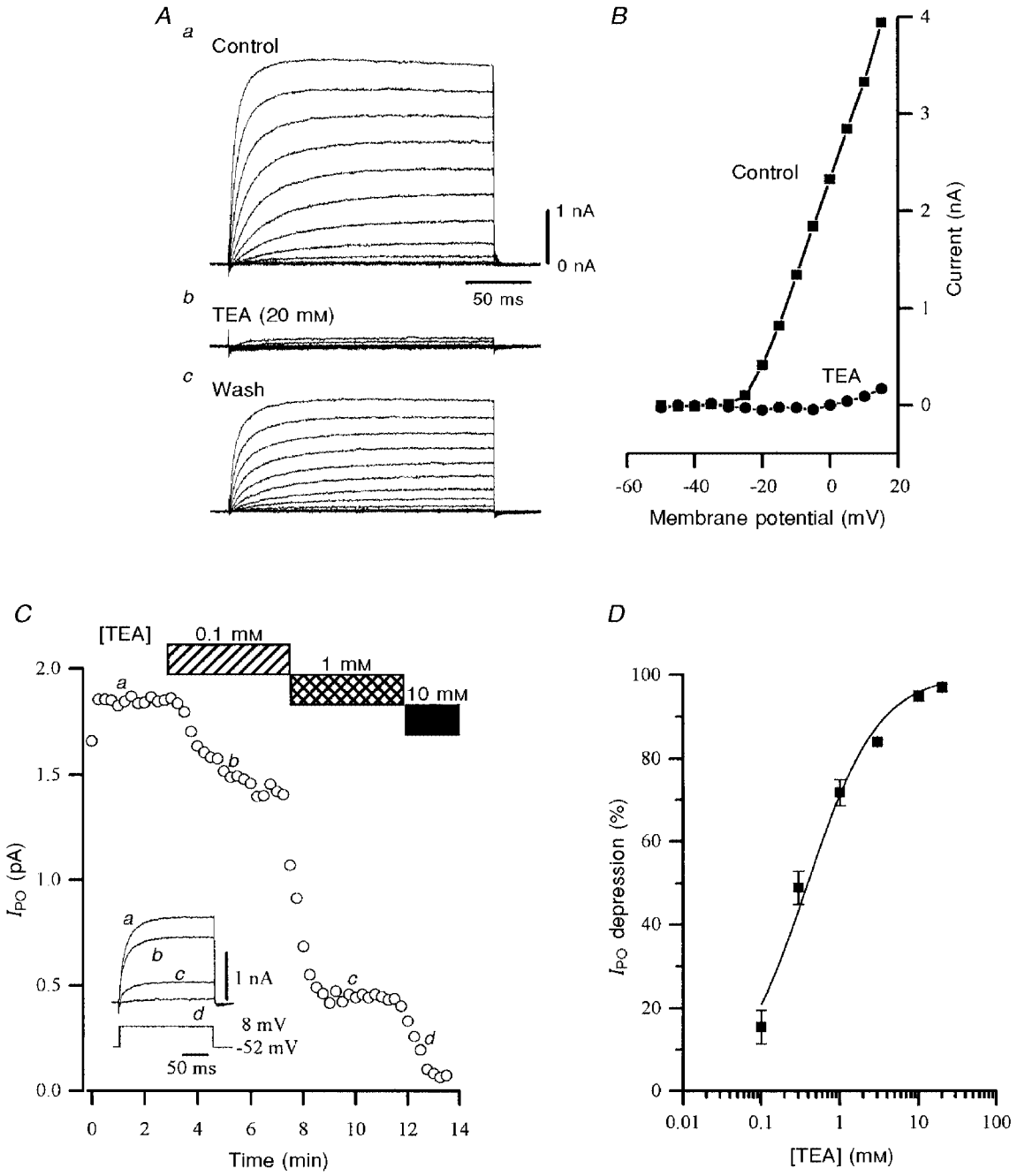

Figure 6. I_{PO} is sensitive to block by TEA

A, outward currents resulting from depolarizing steps from −50 to +15 mV in 5 mV increments under control conditions (*a*), in the presence of TEA (20 mM; *b*) and after washout (10 min; *c*). Recordings were made with caesium gluconate-filled pipette solution in low-Ca^{2+} aCSF containing TTX (0·5 μM). *B*, resulting current–voltage relationships from data in *A* for I_{PO} in the absence (■) and presence (●) of TEA (20 mM). Block by TEA appeared to be voltage independent. *C*, plot of I_{PO} amplitude during cumulative application of TEA (0·1, 1 and 10 mM) during the periods denoted by the bars. Inset shows single leak-subtracted current records (upper panel), corresponding to points *a*–*d*, which were evoked every 15 s by 200 ms voltage steps from −52 to +8 mV (lower panel). Recordings were made using caesium gluconate-based pipette solutions, in low-Ca^{2+} aCSF containing TTX (0·5 μM). Not shown is a 1 s conditioning step to −82 mV that preceded a 1 s step to −52 mV, from which the test depolarization was then made. *D*, concentration–effect curve for the depression of I_{PO} by TEA pooled from 6 experiments such as that in *A*. Each point represents the mean data from 3 cells, recorded from different slices. The logarithmic curve fitted to the data had a slope value of 0·97, and gave an IC_{50} for TEA of 0·39 mM.

such that at somatic potentials sufficient to activate all proximal channels, other more distal channels might still not be activated. As these reach activation threshold they would thus contribute to a steadily increasing conductance value. Indeed, even approaching +100 mV an asymptote was not obtained (data not shown). As the activation curve in Fig. 7*B* became linear at potentials positive to a mean value of +35 mV, we took this as the potential at which G_{PO} (at least within the soma) was maximal, at which it was $37{\cdot}8 \pm 1{\cdot}9$ nS. The Boltzmann fit gave half-maximal activation at −5 mV.

Kinetics of I_{PO}

In order to facilitate the study of the activation kinetics of I_{PO}, caesium gluconate-based pipette solutions were used, with an extracellular medium containing zero K^+ and 5 mM Cs^+ ($n = 3$). The time constant (τ) was calculated from a single exponential fit to the peak of the current data, using non-leak-subtracted current to avoid the possibility of leak subtraction distorting the kinetics. The estimated τ for activation decreased from approximately 28 to 8 ms in the range −22 to +13 mV ($n = 3$; Fig. 8*A*), predicting significant I_{PO} activation during the depolarizing phase of an action potential.

The voltage dependence of deactivation was quantified by examination of tail currents recorded using intracellular potassium gluconate and extracellular K^+ (5 mM) at room temperature, in aCSF additionally containing ZD7288 (50 μM). Cells were depolarized from around −50 mV to between −10 and −16 mV for 450 ms, and then hyperpolarized in 5 mV incremental steps (Fig. 8*B*). The currents were leak subtracted and the tails could be well fitted using a single exponential function. Data pooled from four cells indicated that τ decreased linearly with hyperpolarization, being approximately 2 ms at around −60 mV (Fig. 8*B*), showing that I_{PO} deactivates rapidly at around resting membrane potential.

To study inactivation the membrane potential was held at between −60 and −50 mV and stepped (for up to 4 s) in depolarizing increments up to around +50 mV (using caesium gluconate-based pipette solutions and either extracellular Cs^+ (5 mM; $n = 3$) or K^+ (2·5 mM; $n = 3$)). Inactivation of I_{PO} was very slow and could not be well fitted by a single exponential function (Fig. 9*A*). In an attempt to quantify the inactivation, the peak current amplitude was divided by the current amplitude 3 s after the peak. This 'inactivation ratio' (which was $1{\cdot}66 \pm 0{\cdot}14$ at $+22{\cdot}3 \pm 0{\cdot}3$ mV; $n = 4$) appeared to be unrelated to membrane potential (Fig. 9*Ab*). The slow inactivation of I_{PO} that developed during a 1 s depolarizing step to around +10 mV could be relieved following interruption by brief (20–200 ms duration) hyperpolarizing steps to potentials in the range 0 to −100 mV (Fig. 9*B*). The greater the amplitude of the hyperpolarizing steps, the greater the deinactivation. Thus, for 20 ms steps to −90 and −60 mV, the ratios of peak pre-step (non-inactivated) current to peak post-step (deinactivated) current were $1{\cdot}11 \pm 0{\cdot}03$ and $1{\cdot}20 \pm 0{\cdot}03$, respectively ($n = 5$ in each case; $P < 0{\cdot}01$ by Student's paired t test). In addition, longer hyperpolarizing steps gave greater relief from inactivation (Fig. 9*B*), such that steps to −90 mV for 20 or 200 ms resulted in peak control/peak test current ratios of $1{\cdot}11 \pm 0{\cdot}03$ and $0{\cdot}99 + 0{\cdot}02$, respectively ($n = 5$; $P < 0{\cdot}01$ by Student's paired t test). This relief of inactivation by brief hyperpolarization suggests that inactivation is a property of the channels carrying I_{PO}, rather than due to

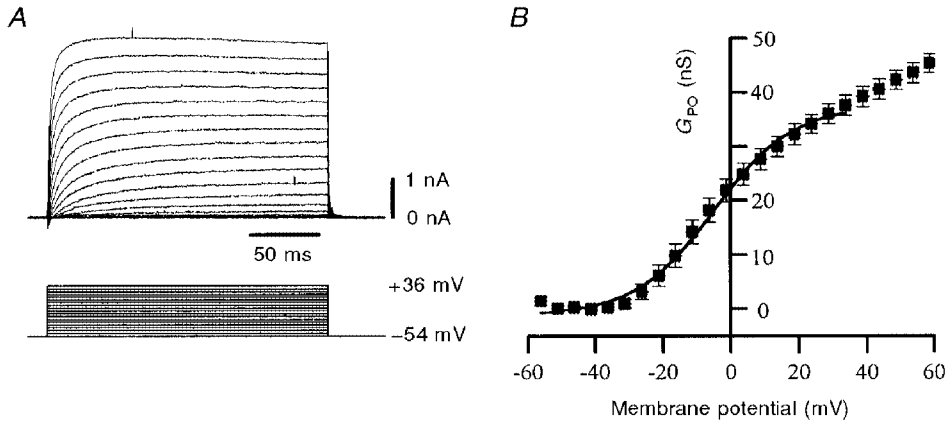

Figure 7. Voltage dependence of I_{PO} activation

A, a family of leak-subtracted I_{PO} (upper panel) evoked using the voltage protocol (5 mV increments) shown in the lower panel. The cell was recorded with caesium gluconate-based pipette solution in low-Ca^{2+} aCSF containing TTX (0·5 μM) and Cs^+ (10 mM), with zero K^+. *B*, plot of data pooled from 6 such experiments, with points representing means ± S.E.M. of both I_{PO} conductance and membrane potential. Leak-subtracted current data from experiments such as those in *A* were normalized for driving force by dividing by $V - E_{Cs}$, with E_{Cs} derived from that predicted by the Nernst equation. Data points were fitted with a Boltzmann function, assuming maximal somatic I_{PO} activation at +35 mV (see text). Half-maximal activation was at −5 mV, with the threshold at around −30 mV.

gradual extracellular ion accumulation reducing the driving force on the permeant ion.

Influence of I_{PO} on action potential generation

We sought to identify the role played by I_{PO} in influencing the behaviour of SThN neurones in current-clamp mode by using TEA (1 mM), which would be expected to block I_{PO} by around 80%. TEA (1 mM) caused a pronounced block of the initial phase of the action potential after-hyperpolarization, and also increased the action potential duration by around 50% (Fig. 10*A*). This was in contrast to low-Ca^{2+} aCSF, which was without effect on either of these variables (not shown), indicating that this effect was not due to an action of TEA upon I_C, the TEA-sensitive Ca^{2+}-dependent K^+ current mediated by high-conductance Ca^{2+}-sensitive K^+ (BK) channels (Pennefather *et al.* 1985; Lo *et al.* 1998). When sustained high-frequency action potential firing was induced by a series of depolarizing current injection steps (300 ms), under control conditions spike frequency adaptation was minimal (see also Bevan & Wilson, 1999), and accommodation was only observed with sustained firing at frequencies higher than around 350 Hz (Fig. 10*B*). However, in TEA (1 mM), firing rates in excess of around 200 Hz could not be sustained, due to accommodation, for more than a few tens of milliseconds (Fig. 10*B*). These results suggest that I_{PO} contributes to the brisk repolarization of the action potential, and that this in turn aids sodium channel deinactivation which is necessary to permit sustained firing at frequencies above around 200 Hz without accommodation.

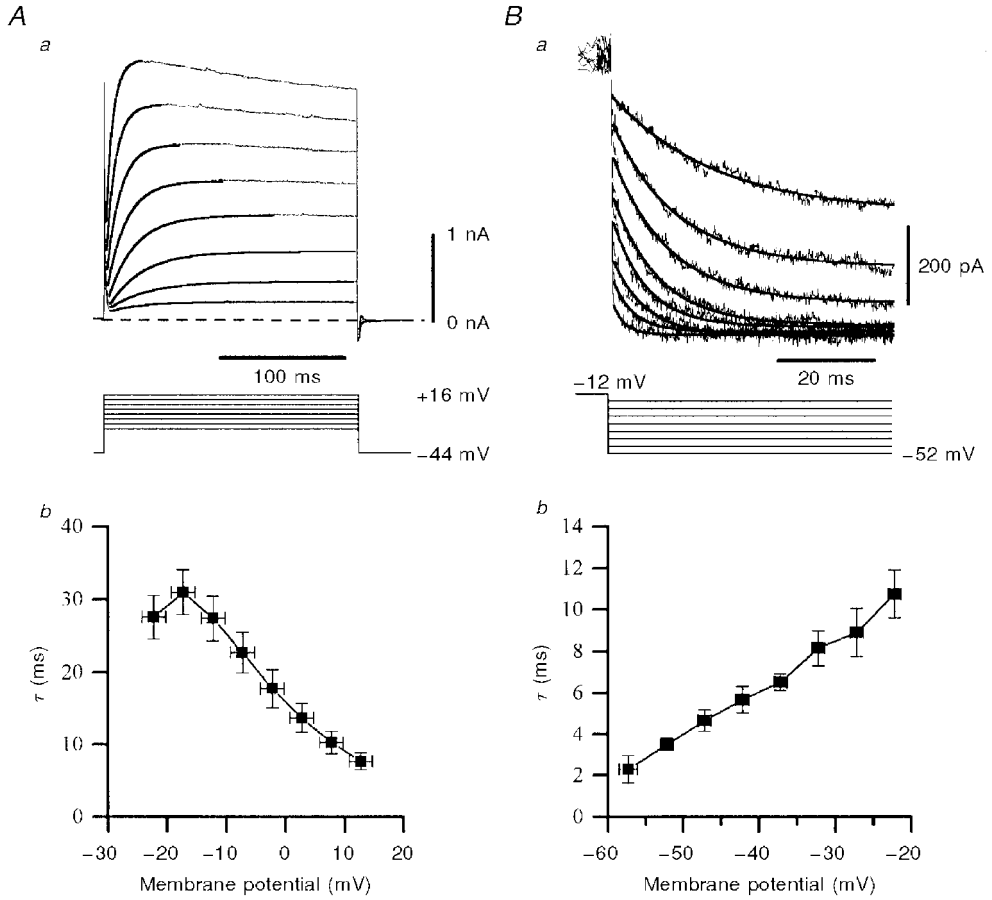

Figure 8. Activation and deactivation kinetics of I_{PO}

A, activation. *Aa*, example of a family of currents (upper panel) generated by depolarizing steps (lower panel), from which activation kinetics were derived. Single exponential fits (thick overlays) were made to the peak of the rising phase of the currents (not leak-subtracted) to extract the time constant (τ). Cell recorded with a caesium gluconate-filled pipette in low-Ca^{2+} aCSF containing TTX (0·5 μM) and Cs^+ (5 mM). *Ab*, data pooled from 3 such cells showing the relationship between the activation time constant τ and membrane potential. The greater the depolarization, the more rapidly I_{PO} activated. *B*, deactivation. *Ba*, leak-subtracted I_{PO} tails from a single cell (upper panel) resulting from a series of hyperpolarizing steps from −12 mV (lower panel), preceded by holding at −12 mV for 500 ms (to inactivate any transient currents; not shown). Cell recorded with a potassium gluconate-filled pipette at room temperature in low-Ca^{2+} aCSF containing ZD7288 (50 μM), TTX (0·5 μM) and K^+ (5 mM). Tail currents were well fitted by a single exponential function (continuous thick lines). *Bb*, mean values of I_{PO} deactivation time constant τ derived from 4 such experiments. The greater the membrane repolarization, the faster I_{PO} deactivated.

DISCUSSION

Distinctive characteristics of I_{PO}

We have demonstrated that rat SThN neurones possess a rapidly activating, very slowly inactivating, outwardly rectifying 'persistent outward' K^+ current that activates positive to around −30 mV, which we have termed I_{PO}. Other membrane currents active in this range of membrane potentials were abolished by blockers of voltage-gated Ca^{2+} and Na^+ channels or, in the case of transient A-like K^+ currents, either by exploiting their rapid inactivation at potentials positive to around −60 mV, or by intracellular dialysis with Cs^+. Indeed, after 500 ms at membrane potentials positive to around −16 mV, there appears to be only a single component of voltage-dependent membrane current active, as the tail currents seen on repolarization could be fitted by a single exponential function, even with potassium gluconate-containing recording pipettes. The dependence of these tail current reversal potentials on $[K^+]_o$ was consistent with I_{PO} being a K^+ current, although there was some deviation from predicted Nernstian behaviour, particularly at lower $[K^+]_o$. This might be because (1) any extracellular accumulation of extruded K^+ ions through the channel will tend to shift the reversal potential in a positive direction; this would be (and was) particularly evident with low $[K^+]_o$. (2) In low $[K^+]_o$ the currents reverse at potentials at which I_{PO} deactivation is most rapid, compromising accurate measurement of current amplitude. In addition, the reversal potentials could be influenced by weak permeability of the channel to other ions, and to an influence of incomplete block of other currents.

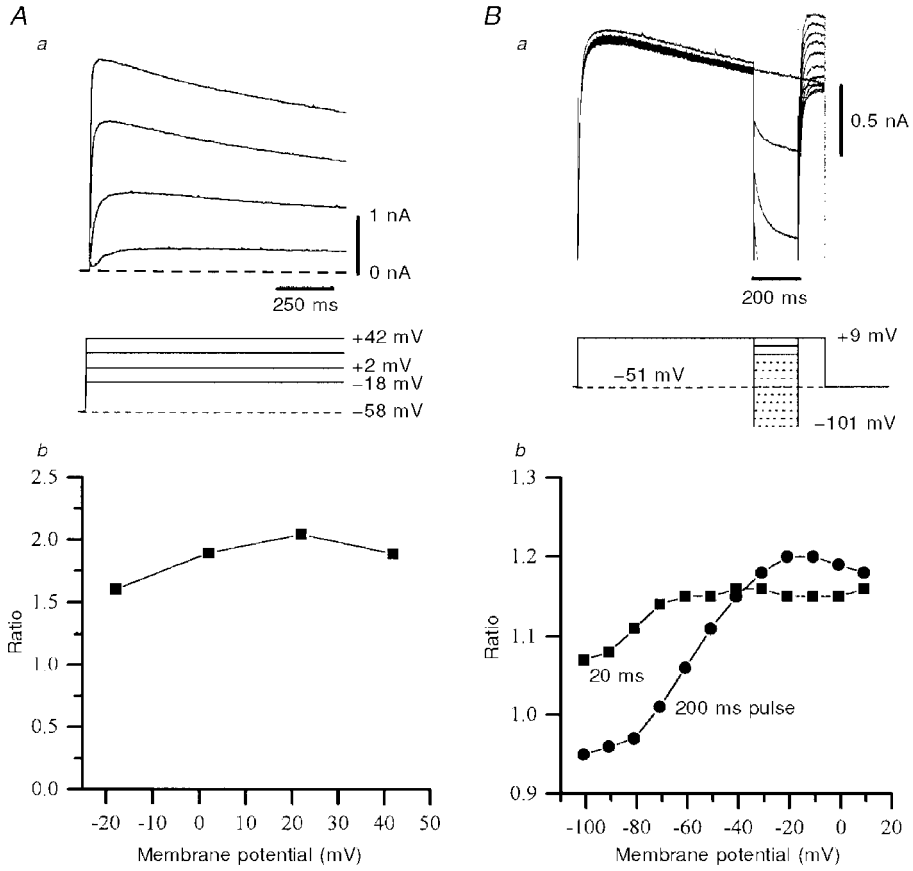

Figure 9. Inactivation and deinactivation kinetics of I_{PO}

Aa, non-exponential inactivation of I_{PO} could be observed (upper panel; not leak subtracted) during sustained depolarizing voltage steps (lower panel). Recording made with a caesium gluconate-filled pipette in low-Ca^{2+} aCSF containing TTX (0·5 μM) and Cs^+ (5 mM); only the first 1 s of the step is shown. *Ab*, the ratio of peak current to current at 3 s after the peak for the cell in *Aa* showed no clear relationship to membrane potential. *B*, the inactivation of I_{PO} can be relieved by hyperpolarization. *Ba*, upper panel: overlaid currents from 12 trials, each consisting of an inactivating control (pre-step) current, interrupted by a transient hyperpolarizing step (200 ms) of varying magnitude. Currents truncated negative to +0·5 nA. Lower panel: voltage protocol, where dashed lines represent steps producing the currents that are truncated in the upper panel. *Bb*, plot of the ratio of peak pre-step current to peak post-step current *vs.* the step potential for steps of 20 (■) and 200 ms (●) duration from the cell in *Ba*. Deinactivation is more apparent the greater the amplitude and duration of the hyperpolarizing step. Relief from inactivation (ratio = 1) occurred at around −70 mV for a 200 ms step. Currents were not leak subtracted.

On discovering that intracellular dialysis with Cs^+ did not affect I_{PO}, this condition was used to study several of the other properties of I_{PO} of interest because of block of A-type currents, and the possibility of better voltage control. Indeed, under conditions in which both intracellular and extracellular K^+ were nominally replaced by Cs^+, I_{PO} current tails displayed a near-Nernstian dependence upon $[Cs^+]_o$, confirming the channel's ability to conduct Cs^+. While Cs^+ permeability of K^+ channels is not commonly observed, there are precedents for this in slowly inactivating outwardly rectifying currents in other cell types, such as the avian nucleus magnocellularis (Rathouz & Trussell, 1998), bullfrog sympathetic neurones (Block & Jones, 1997), chick dorsal root ganglion neurones (Trequattrini *et al.* 1996) and in cells expressing human Kv1.5 channels (Fedida *et al.* 1999). Many other outwardly rectifying K^+ currents described elsewhere display block by TEA, Ba^{2+} and 4-AP, as shown for I_{PO}. However, the high sensitivity of I_{PO} to block by extracellular TEA, with an IC_{50} of around 0·4 mM, is particularly noteworthy, resembling instances of slowly inactivating outwardly rectifying currents with IC_{50} values for TEA block in the range 0·1–1 mM reported in the neurones of medial nucleus of the trapezoid body (Brew & Forsythe, 1995; Wang *et al.* 1998*b*), thalamic relay neurones (Huguenard & Prince, 1991), globus pallidus (Baranauskas *et al.* 1999) and in cortical (Erisir *et al.* 1999) and hippocampal (Martina *et al.* 1998) interneurones.

The kinetic analysis of I_{PO} is likely to be compromised by neuronal geometry, and the potential difficulty in voltage clamping distal parts with sufficient rapidity. However, under the conditions used, it proved possible to fit the kinetics of both activation and deactivation by a single exponential function, minimizing such concerns. The voltage dependence of the activation time constant decreased as the membrane

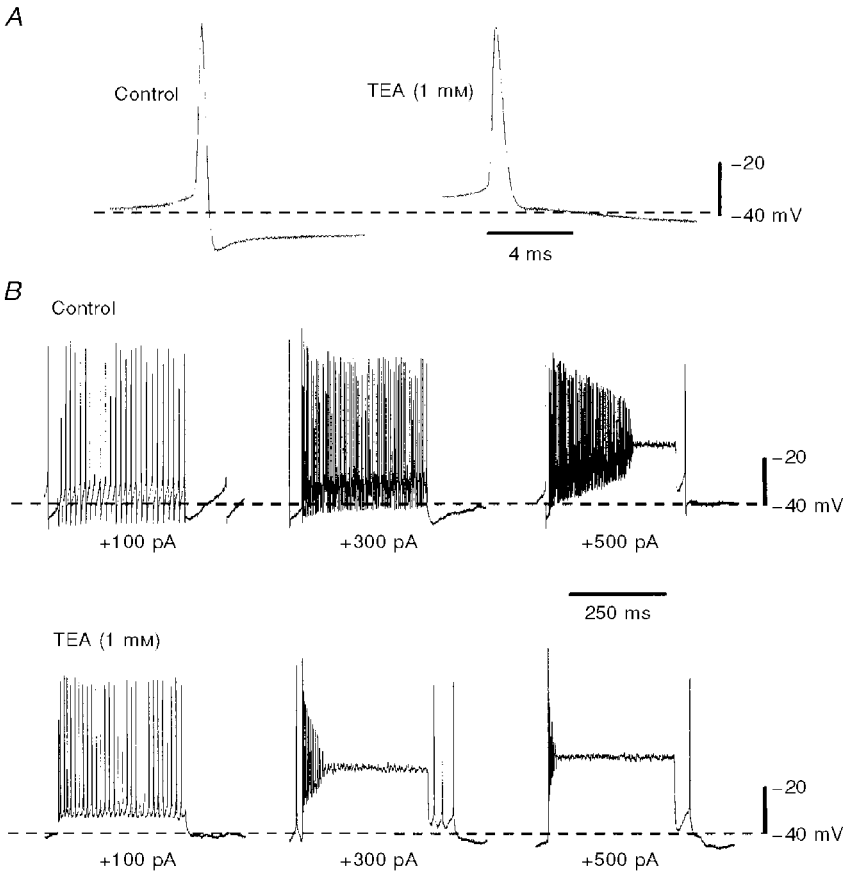

Figure 10. TEA, at a concentration (1 mM) expected to block I_{PO} by around 80%, affects single spike characteristics and increases accommodation at high firing frequencies

A, two action potentials from the same cell, showing an increase in duration, and reduction in after-hyperpolarization amplitude, in TEA (1 mM). *B*, TEA (1 mM) impairs high-frequency action potential firing by enhancing accommodation. Two sets of records of membrane potential from the same cell in control conditions (upper records) and in TEA (1 mM; lower records). Records show, for both conditions, the result of injecting depolarizing current (100, 300 and 500 pA) for 300 ms while the cell was at rest. Higher frequencies of action potential firing thus elicited could be better sustained under control conditions (200 Hz, middle panel; initially around 300 Hz in right-hand panel), whereas TEA promoted accommodation, supporting a role for I_{PO} in action potential repolarization and consequent sodium channel deinactivation.

was stepped to more depolarized potentials, and at the peak of an action potential, where the activation time constant τ will be less than 10 ms (at 32 °C), I_{PO} would be expected to activate significantly. Deactivation was also both fast and voltage dependent, with a time constant of approximately 2 ms at −60 mV (at room temperature). Thus, while it would be predicted that I_{PO} would contribute to action potential repolarization, its influence would be short-lived on the return of the membrane potential to rest, and thus would not impair generation of subsequent action potentials, as long as the interspike interval was in excess of 2–3 ms. I_{PO} inactivation was very slow and non-exponential and, given that in a spontaneously active neurone I_{PO} will serve to repolarize the cell and thus not permit inactivation to occur, this characteristic is unlikely to be of great physiological relevance. However, as it could be reversed by a transient deinactivating hyperpolarization, inactivation does appear to be a real property of the current. Again, the voltage dependence and kinetic features of I_{PO} are comparable to other relatively non-inactivating outward rectifiers described in the neurones of medial nucleus of the trapezoid body (Brew & Forsythe, 1995; Wang *et al.* 1998*b*), avian nucleus magnocellularis (Rathouz & Trussell, 1998), thalamic relay neurones (Huguenard & Prince, 1991), islands of Calleja (Halliwell & Horne, 1995), globus pallidus (Baranauskas *et al.* 1999), and interneurones in cortex (Erisir *et al.* 1999) and hippocampus (Martina *et al.* 1998).

I_{PO} is likely to result from expression of Kv3.1

Outwardly rectifying K^+ channels can be formed from a number of gene families, namely *Kv1*, *Kv2*, *Kv3*, *eag* (*ether-à-go-go*) and *KCNQ* (Pongs, 1992; Shi *et al.* 1997, 1998; Robertson, 1997; Wang *et al.* 1998*a*), although their properties can be complicated by the coexpression of heteromers or auxiliary subunits (Robertson, 1997; Mathie *et al.* 1998; Blaine & Ribera, 1998). Nonetheless, in seeking a molecular correlate for the channels carrying I_{PO}, Kv2, eag and KCNQ are unlikely candidates due to differences in their kinetics and/or TEA sensitivity (Pongs, 1992; Shi *et al.* 1997, 1998; Robertson, 1997; Wang *et al.* 1998*a*). Message encoding members of both the Kv1 and Kv3 families has been detected in the SThN (Perney *et al.* 1992; Weiser *et al.* 1994; Verma-Kurvari *et al.* 1997). As both Kv1 and Kv3 channels show relatively fast deactivation kinetics and TEA sensitivity it is harder to differentiate conclusively between them. However, it has been suggested, for Kv1.1, 1.2, 1.3 and 1.5 at least, that their deactivation time constants at −60 mV are in the order of 15–40 ms (Grissmer *et al.* 1994), an order of magnitude greater than that of I_{PO}. In contrast, the deactivation time constant of Kv3.1 is 1–2 ms at −60 mV (Grissmer *et al.* 1994; Hernández-Pineda *et al.* 1999), very similar to that of I_{PO}. Our estimate of 0·39 mM for the IC_{50} of TEA on I_{PO} can be compared favourably with that reported in expressed Kv3.1 channels (~0·3 mM, Grissmer *et al.* 1994; 0·38 mM, Hernández-Pineda *et al.* 1999), as well as their relatively low inactivation. However, it remains possible that I_{PO} is mediated by other members of the Kv3 family, possibly heteromerically expressed with Kv3.1 (Weiser *et al.* 1994).

Possible role of I_{PO} in SThN neurones

Kv3.1 in particular has been associated with 'fast spiking neurones' able to sustain high rates of firing activity (Martina *et al.* 1998; Wang *et al.* 1998*b*; Baranauskas *et al.* 1999; Hernández-Pineda *et al.* 1999) by virtue of its activation at depolarized levels and fast deactivation. Indeed, SThN neurones are also capable of firing at high rates and we have shown that TEA (1 mM), a concentration expected to block I_{PO}, and Kv3.1, by about 80%, has a profound effect on the firing activity, by blocking the fast after-hyperpolarization and permitting accommodation at higher firing rates. These effects of TEA confirm predictions of the effect of block of I_{PO} based upon its kinetics. Such a role in accelerating action potential repolarization, and reducing its duration, has previously been attributed to Kv3.1 in other cell types (Du *et al.* 1996; Whim & Kaczmarek, 1998; Wang *et al.* 1998*b*; Erisir *et al.* 1999). In demonstrating sensitivity of both action potential repolarization and spike frequency adaptation to 1 mM TEA, it is tempting to conclude that this reflects the result of a selective block of I_{PO} by TEA at this particular concentration. However, while targeting of BK channels by TEA may be discounted, the possibility of channels of the Kv1 family (Verma-Kurvari *et al.* 1997) and/or other as yet unidentified TEA-sensitive channels being expressed in SThN neurones renders it prudent to be circumspect about attributing all the effects of TEA shown here to block of I_{PO}/Kv3.1. Nonetheless, the finding that the block of conductance(s) sensitive to 1 mM TEA prevents sustained firing at frequencies greater than around 200 Hz is very much in line with observations made in neurones of the medial nucleus of the trapezoid body, which were attributed solely to an effect on Kv3.1 (Wang *et al.* 1998*b*), and qualitatively similar to those made in cortical interneurones, also attributed to a block of Kv3.1/Kv3.2 channels by TEA (Erisir *et al.* 1999).

The SThN and the globus pallidus appear to be functionally linked, either by reciprocal interconnectivity or co-activation by common inputs (Plenz & Kitai, 1999; Magill *et al.* 2000). SThN and globus pallidus neurones can both sustain high rates of firing, and exhibit high-frequency burstiform activity, both in association with normal information processing in the basal ganglia and particularly during the aberrant activity associated with parkinsonian akinesia (Wichmann & Delong, 1996). Demonstration of similar currents to I_{PO}, subserved by Kv3 channels, in neurones of the globus pallidus (Baranauskas *et al.* 1999; Hernández-Pineda *et al.* 1999) indicates that expression of Kv3 K^+ channels enables this high-frequency activity in both the SThN and globus pallidus. This property is critical to the function of neurones in both these regions and thence in shaping the output of the basal ganglia as a whole.

Albin, R. L., Young, A. B. & Penney, J. B. (1989). The functional anatomy of basal ganglia disorders. *Trends in Neurosciences* **12**, 366–375.

Alexander, G. E., Crutcher, M. D. & Delong, M. R. (1990). Basal ganglia-thalamocortical circuits: parallel substrates for motor, oculomotor, 'prefrontal' and 'limbic' functions. *Progress in Brain Research* **85**, 119–146.

Baranauskas, G., Tkatch, T. & Surmeier, D. J. (1999). Delayed rectifier currents in rat globus pallidus neurons are attributable to Kv2.1 and Kv3.1/3.2 K^+ channels. *Journal of Neuroscience* **19**, 6394–6404.

Benazzouz, A., Gross, C., Feger, J., Boraud, T. & Bioulac, B. (1993). Reversal of rigidity and improvement of motor performance by subthalamic high-frequency stimulation in MPTP-treated monkeys. *European Journal of Neuroscience* **5**, 382–389.

Bergman, H., Wichmann, T. & Delong, M. R. (1990). Reversal of experimental Parkinsonism by lesions of the subthalamic nucleus. *Science* **249**, 1436–1438.

Bergman, H., Wichmann, T., Karmon, B. & Delong, M. R. (1994). The primate subthalamic nucleus. II. Neuronal activity in the MPTP model of parkinsonism. *Journal of Neurophysiology* **72**, 507–520.

Beurrier, C., Congar, P., Bioulac, B. & Hammond, C. (1999). Subthalamic nucleus neurons switch from single-spike activity to burst-firing mode. *Journal of Neuroscience* **19**, 599–609.

Bevan, M. D. & Wilson, C. J. (1999). Mechanisms underlying spontaneous oscillation and rhythmic firing in rat subthalamic neurons. *Journal of Neuroscience* **19**, 7617–7628.

Blaine, J. T. & Ribera, A. B. (1998). Heteromultimeric potassium channels formed by members of the Kv2 subfamily. *Journal of Neuroscience* **18**, 9585–9593.

Block, B. M. & Jones, S. W. (1997). Delayed rectifier current of bullfrog sympathetic neurons: ion–ion competition, asymetrical block and effects of ions on gating. *Journal of Physiology* **499**, 403–416.

Brew, H. M. & Forsythe, I. D. (1995). Two voltage-dependent K^+ conductances with complementary functions in postsynaptic integration at a central auditory synapse. *Journal of Neuroscience* **15**, 8011–8022.

Brown, P. & Marsden, C. D. (1998). What do the basal ganglia do? *Lancet* **351**, 1801–1804.

Delong, M. R. (1990). Primate models of movement disorders of basal ganglia origin. *Trends in Neurosciences* **13**, 281–285.

Du, J., Zhang, L., Weiser, M., Rudy, B. & McBain, C. J. (1996). Developmental expression and functional characterization of the potassium-channel subunit Kv3.1b in parvalbumin-containing interneurons of the rat hippocampus. *Journal of Neuroscience* **16**, 506–518.

Erisir, A., Lau, D., Rudy, B. & Leonard, C. S. (1999). Function of specific K^+ channels in sustained high-frequency firing of fast-spiking neocortical interneurons. *Journal of Neurophysiology* **82**, 2476–2489.

Fedida, D., Maruoka, N. D. & Lin, S. (1999). Modulation of slow inactivation in human cardiac Kv1.5 channels by extra- and intracellular permeant cations. *Journal of Physiology* **515**, 315–329.

Grissmer, S., Nguyen, A. N., Aiyar, J., Hanson, D. C., Mather, R. J., Gutman, G. A., Karmilowicz, M. J., Auperin, D. D. & Chandy, K. G. (1994). Pharmacological characterization of five cloned voltage-gated K^+ channels, types Kv1.1, 1.2, 1.3, 1.5, and 3.1, stably expressed in mammalian cell lines. *Molecular Pharmacology* **45**, 1227–1234.

Guridi, J. & Obeso, J. A. (1997). The role of the subthalamic nucleus in the origin of hemiballism and parkinsonism: New surgical perspectives. *Advances in Neurology* **74**, 235–247.

Halliwell, J. V. & Horne, A. L. (1995). Membrane properties of the granule cells of the islands of Calleja of the rat studied *in vitro*. *Journal of Physiology* **487**, 421–440.

Hassani, O. K., Mouroux, M. & Féger, J. (1996). Increased subthalamic neuronal activity after nigral dopaminergic lesion independent of disinhibition via the globus pallidus. *Neuroscience* **72**, 105–115.

Hernández-Pineda, R., Chow, A., Amarillo, Y., Moreno, H., Saganich, M., Vega-Saenz de Miera, E., Hernández-Cruz, A. & Rudy, B. (1999). Kv3.1-Kv3.2 channels underlie a high-voltage-activating component of the delayed rectifier K^+ current in projecting neurons from the globus pallidus. *Journal of Neurophysiology* **82**, 1512–1528.

Huguenard, J. R. & Prince, D. A. (1991). Slow inactivation of a TEA-sensitive K^+ current in acutely isolated rat thalamic relay neurons. *Journal of Neurophysiology* **66**, 1316–1328.

Krack, P., Hamel, W., Mehdorn, H. M. & Deuschl, G. (1999). Surgical treatment of Parkinson's disease. *Current Opinion in Neurology* **12**, 417–425.

Limousin, P., Pollak, P., Benazzouz, A., Hoffmann, D., Le Bas, J.-F., Broussolle, E., Perret, J. E. & Benabid, A.-L. (1995). Effect on parkinsonian signs and symptoms of bilateral subthalamic nucleus stimulation. *Lancet* **345**, 91–95.

Lo, F. S., Cork, R. J. & Mize, R. R. (1998). Physiological properties of neurons in the optic layer of the rat's superior colliculus. *Journal of Neurophysiology* **80**, 331–343.

Magill, P., Bolam, J. P. & Bevan, M. D. (2000). Relationship of activity in the subthalamic nucleus-globus pallidus network to cortical electroencephalogram. *Journal of Neuroscience* **20**, 820–833.

Martina, M., Schultz, J. H., Ehmke, H., Monyer, H. & Jonas, P. (1998). Functional and molecular differences between voltage-gated K^+ channels of fast-spiking interneurons and pyramidal neurons of rat hippocampus. *Journal of Neuroscience* **18**, 8111–8125.

Mathie, A., Wooltorton, J. R. A. & Watkins, C. S. (1998). Voltage-activated potassium channels in mammalian neurons and their block by novel pharmacological agents. *General Pharmacology* **30**, 13–24.

Matsumara, M., Kojima, J., Gardner, T. & Hikosaka, O. (1992). Visual and oculomotor functions of monkey subthalamic nucleus. *Journal of Neurophysiology* **67**, 1615–1632.

Miyazaki, T. & Lacey, M. G. (1998). Presynaptic inhibition by dopamine of a discrete component of GABA release in rat substantia nigra pars reticulata. *Journal of Physiology* **513**, 805–817.

Nakanishi, H., Kita, H. & Kitai, S. T. (1987). Electrical membrane properties of rat subthalamic neurons in an *in vitro* slice preparation. *Brain Research* **437**, 35–44.

Parent, A. & Hazrati, L.-N. (1995). Functional anatomy of the basal ganglia. I. The cortico-basal ganglia-thalamo-cortical loop. *Brain Research Reviews* **20**, 91–127.

Pennefather, P. S., Lancaster, B., Adams, P. R. & Nicoll, R. A. (1985). Two distinct Ca-dependent K currents in bullfrog sympathetic ganglion cells. *Proceedings of the National Academy of Sciences of the USA* **82**, 3040–3044.

Perney, T. M., Marshall, J., Martin, K. A., Hockfield, S. & Kaczmarek, L. K. (1992). Expression of the mRNAs for the Kv3.1 potassium channel gene in the adult and developing rat brain. *Journal of Neurophysiology* **68**, 756–766.

Plenz, D. & Kitai, S. T. (1999). A basal ganglia pacemaker formed by the subthalamic nucleus and external globus pallidus. *Nature* **400**, 677–682.

Pongs, O. (1992). Molecular biology of voltage-dependent potassium channels. *Physiological Reviews* **72**, S69–S88.

Rathouz, M. & Trussell, L. (1998). Characterization of outward currents in neurons of the avian nucleus magnocellularis. *Journal of Neurophysiology* **80**, 2824–2835.

Robertson, B. (1997). The real life of voltage-gated K^+ channels: more than model behaviour. *Trends in Pharmacological Sciences* **18**, 474–483.

Shi, W., Wang, H.-S., Pan, Z., Wymore, R. S., Cohen, I. S., McKinnon, D. & Dixon, J. E. (1998). Cloning of a mammalian *elk* potassium channel gene and EAG mRNA distribution in rat sympathetic ganglia. *Journal of Physiology* **511**, 675–682.

Shi, W., Wymore, R. S., Wang, H. S., Pan, Z., Cohen, I. S., McKinnon, D. & Dixon, J. E. (1997). Identification of two nervous system-specific members of the erg potassium channel gene family. *Journal of Neuroscience* **17**, 9423–9432.

Trequattrini, C., Petris, A. & Franciolini, F. (1996). Characterization of a neuronal delayed rectifier K current permeant to Cs and blocked by verapamil. *Journal of Membrane Biology* **154**, 143–153.

Verma-Kurvari, S., Border, B. & Joho, R. H. (1997). Regional and cellular expression patterns of four K^+ channel mRNAs in the adult rat brain. *Molecular Brain Research* **46**, 54–62.

Wang, H. S., Pan, Z., Shi, W., Brown, B. S., Wymore, R. S., Cohen, I. S., Dixon, J. E. & McKinnon, D. (1998*a*). KCNQ2 and KCNQ3 potassium channel subunits: molecular correlates of the M-channel. *Science* **282**, 1890–1893.

Wang, L.-Y., Gan, L., Forsythe, I. D. & Kaczmarek, L. K. (1998*b*). Contribution of the Kv3.1 potassium channel to high-frequency firing in mouse auditory neurones. *Journal of Physiology* **509**, 183–194.

Weiser, M., Vega-Saenz de Miera, E., Kentros, C., Moreno, H., Franzen, L., Hillman, D., Baker, H. & Rudy, B. (1994). Differential expression of Shaw-related K^+ channels in the rat central nervous system. *Journal of Neuroscience* **14**, 949–972.

Whim, M. D. & Kaczmarek, L. K. (1998). Heterologous expression of the $K_v3.1$ potassium channel eliminates spike broadening and the induction of a depolarizing afterpotential in the peptidergic bag cell neurons. *Journal of Neuroscience* **18**, 9171–9180.

Wichmann, T., Bergman, H. & Delong, M. R. (1994*a*). The primate subthalamic nucleus. I. Functional properties in intact animals. *Journal of Neurophysiology* **72**, 494–506.

Wichmann, T., Bergman, H. & Delong, M. R. (1994*b*). The primate subthalamic nucleus. III. Changes in motor behavior and neuronal activity in the internal pallidum induced by subthalamic inactivation in the MPTP model of parkinsonism. *Journal of Neurophysiology* **72**, 521–530.

Wichmann, T. & Delong, M. R. (1996). Functional and pathophysiological models of the basal ganglia. *Current Opinion in Neurobiology* **6**, 751–758.

Wigmore, M. A. & Lacey, M. G. (1999). Characterisation of a persistent outward current that can be carried by Cs^+ in rat subthalamic nucleus neurones *in vitro*. *Journal of Physiology* **521.P**, 93*P*.

Acknowledgements

We are grateful to the Wellcome Trust for their support (grant number 050222).

Corresponding author

M. G. Lacey: Department of Pharmacology, Division of Neuroscience, The Medical School, University of Birmingham, Vincent Drive, Edgbaston, Birmingham B15 2TT, UK.

Email: m.g.lacey@bham.ac.uk